Catalysis Today 143 (2009) 115–119

Contents lists available at ScienceDirect

Catalysis Today

journal homepage: www.elsevier.com/locate/cattod

Effect of the support acidity on the aromatic ring-opening of pyrolysis gasoline over Pt/HZSM-5 catalysts

Pedro Castaño [a], Alazne Gutiérrez [a], Inés Villanueva [a], Barbara Pawelec [b], Javier Bilbao [a], Jose M. Arandes [a,*]

[a] Universidad del País Vasco, Dpto. Ingeniería Química, Apdo. 644, 48080 Bilbao, Spain
[b] Instituto de Catálisis y Petroleoquímica, CSIC, c/Marie Curie 2, Cantoblanco, 28049 Madrid, Spain

ARTICLE INFO

Article history:
Available online 19 December 2008

Keywords:
Platinum
HZSM-5
Noble metal catalyst
Hydrocracking
Aromatic ring-opening
Deactivation
Pyrolysis gasoline

ABSTRACT

In this paper we evaluate the effect of the acidity of the support (HZSM-5) and the nature of the interaction between the active phases of the bifunctional Pt/HZSM-5 catalyst on the aromatic ring-opening of pyrolysis gasoline under hydrocracking conditions. The catalysts were characterized by N_2 adsorption–desorption isotherms, CO chemisorption, pyridine FTIR, NH_3 adsorption-DSC and NH_3 TPD. The catalyst screening in the pyrolysis gasoline hydrocracking demonstrated that: (i) the conversion of pyrolysis gasoline is linearly dependent on support acidity. At low acidities values the main mechanisms of ring-opening is through hydrogenolysis and thus, the less acidic catalyst shows higher conversion than expected; (ii) the synergysm between the metal and acid-sites is enhanced when using a bifunctional catalyst instead of a hybrid one, due to the increase in H_2 spill-over efficiency. However, in terms of activity, the most acid catalyst (hybrid) shows the highest aromatic conversion, in correspondence with (i).

1. Introduction

The actual limitations of crude oil reserves [1], together with severer requirements of the fuels imposed by environmental legislations [2], are forcing refineries to use more refractory feedstock while to manufacture less pollutant fuels. Hydrocracking offers an outlet for the valorisation of surplus aromatics emerging from the present situation [1]. In particular, pyrolysis gasoline (PyGas) ring-opening has recently received considerable attention due to its high aromatics content and its intensive production by the petrochemical industry [3]. This feedstock is a by-product of the steam cracker and can be upgraded with the hydrogen produced in the same unit over bifunctional catalysts based on noble metals (Pt, Pd, Ir) on zeolites (HY, HZSM-5, Hβ) [4,5]. The target is producing an alkane-rich feedstock which boosts the production of ethylene when reintroduced to the steam cracker [6].

The properties of the support, in terms of acidity and shape-selectivity, have a great impact on product selectivity on the individual steps [7] or the direct route [8] of aromatic ring-opening. Besides, the results obtained under severe ring-opening (SRO) conditions indicate a linear dependency of conversion and *n*-alkane yield on total acidity of the catalyst [7,9]. HZSM-5 zeolite offers a suitable two-dimensional pore system, which comprises interconnecting straight (0.56 nm × 0.53 nm) and sinusoidal channels (0.51 nm × 0.55 nm) [10]. This pore network is responsible for favouring monomolecular cracking and inhibition of certain bimolecular cracking reactions, boosting the yield of C_{2+} *n*-alkanes [1,11,12]. Indeed, the majority of the reported work has been conducted using HZSM-5 zeolite [3–5,12,13], whereas the influence of such support and its interaction with the metallic sites remains unclear.

In this paper we have studied the effect of the Pt/HZSM-5 catalyst acidity (by using HZSM-5 zeolites with different Si/Al atomic ratio; 15, 19 and 95) on the activity, selectivity and deactivation during aromatic ring-opening of pyrolysis gasoline under hydrocracking conditions. Additionally, the previous kinetic data will be compared with those obtained under similar conditions using a hybrid catalyst (made by physical mixing of a metallic and acidic function; Pt/γ-Al_2O_3 and HZSM-5 zeolite) and, therefore, the impact of the metal–support interaction on reaction mechanisms will be discussed in detail.

2. Experimental

2.1. Catalyst preparation

Three HZSM-5 zeolites with different Si/Al atomic ratios have been used as supports or acidic functions: Z15 (Si/Al = 15, Zeolyst International); Z19 (Si/Al = 19, Akzo Nobel-Albemarle) and Z95 (Si/Al = 95, Akzo Nobel-Albemarle). Bifunctional Pt/Z15, Pt/Z19 and Pt/

* Corresponding author.
E-mail address: josemaria.arandes@ehu.es (J.M. Arandes).

0920-5861/$ – see front matter © 2008 Elsevier B.V. All rights reserved.
doi:10.1016/j.cattod.2008.10.029

Z95 catalysts were prepared by liquid-phase ion exchange at 60 °C using $Pt(NH_3)_4(NO_3)_2$ as precursor. The volume of the precursor solution required to obtain a platinum loading of 0.5 wt.% was dropwise slowly added to the zeolite suspended in deionized water. The suspension (containing both precursor and zeolite) was stirred for 24 h and then removed under vacuum and 80 °C. After drying at 120 °C for 24 h, the precursors have been ground, sieved ($0.15 < d_p < 0.30$ mm), and calcined at 450 °C for 4 h (heating ramp of 1 °C/min).

Additionally, one hybrid catalyst has been prepared by physical mixing of a metallic function ($Pt/\gamma\text{-}Al_2O_3$ catalyst, Johnson Matthey) with an acidic function (typically used for FCC) named z15 containing HZSM-5 zeolite (Si/Al = 15, 25 wt.%), bentonite (30 wt.%) as binder and $\alpha\text{-}Al_2O_3$ (45 wt.%) as inert charge. This catalyst has been named hereafter as Pt/H15, containing also a proportion of 0.5 wt.% of Pt on pure zeolite basis.

2.2. Catalyst characterization

The metal content of the catalysts was determined by Inductively Coupled Plasma-Atomic Emission Spectroscopy (ICP-AES) using a PerkinElmer Optima 3300DV instrument being the solid sample previously treated with an aqueous solution of HF at 90 °C. Nitrogen adsorption–desorption isotherms were obtained using a Micromeritics ASAP 2010 apparatus, with samples being previously outgassed at 250 °C for 18 h. Metal dispersion was measured by selective CO chemisorption in a Micromeritics ASAP 2010C apparatus. The experimental procedure comprised firstly a 2 h reduction in a flow of H_2 (Alphagaz), followed by pre-treatment under high vacuum (5 h, 10^{-5} mbar) and analysis with CO (Alphagaz, purity of 99.4%) at 35 °C.

Total acidity and acid strength were measured by NH_3 adsorption in a TG-DSC Setaram 111 calorimeter with an attached Harvard syringe pump for the NH_3 injection. The sample was previously heated at 550 °C for 30 min to remove impurities, then the analysis was undertaken at 150 °C by introducing NH_3 (Union Carbide, purity of 99.4%) at a flowrate of 30–40 μL/min. These conditions were used in order to avoid physical adsorption. Once the sample has been completely saturated, the NH_3-TPD was recorded using a quadrupole mass spectrometer (Balzers Quadstar 422), increasing the temperature at a rate of 5 °C/min to 550 °C.

The FTIR measurements were performed in a Nicolet 740 SX FTIR spectrometer with a SPECAC transmittance cell connected to a vacuum pump. The sample weighed 30 mg, being pelletized with KBr, and finally activated under vacuum (30 min) at 300 °C. Pyridine was adsorbed under vacuum at room temperature and the spectrum was recorded at 150 °C. The Brønsted-to-Lewis acid site ratio was calculated from the FTIR vibrational bands of adsorbed pyridine at 1547 cm^{-1} (pyridine-Brønsted) and 1455 cm^{-1} (pyridine-Lewis), using the molar extinction coefficients (pyridine-Brønsted, 1.67 cm/μmol; pyridine-Lewis, 2.22 cm/μmol) reported by Emeis [14].

2.3. Catalytic activity

For the activity test, the supported platinum catalysts (0.2 g) were diluted in 1 g of CSi (0.5 mm previously calcined at 700 °C) and then activated by heating to a reduction temperature of 300 °C in H_2:N_2 mixture (vol. ratio, 1:2), flow rate 90 mL/min at atmospheric pressure, followed by isothermal reduction at this temperature for 2 h.

Hydrocracking of the pyrolysis gasoline was carried out with a continuous down-flow, fixed bed reactor under the following conditions at a temperature range between 350 and 450 °C. Total pressure was varied from 20 to 50 bar keeping a constant gasoline partial pressure of 1 bar and using N_2 to complete the total pressure, if needed. H_2:PyGas molar ratio was varied in the 20–49 range. We observed that, by using these conditions, deactivation is minimized and steady-state data are obtained [8]. The weight hourly space velocity (WHSV) was kept at 4 h^{-1} and a linear velocity along the reactor was maintained at a constant value of 5.77 cm(STP)/s. Product analysis was carried out on-line on a HP5890 Series II GC provided with a FID detector. The method of calculation of pyrolysis gasoline conversion and product distribution has been previously reported [9].

The composition of pyrolysis gasoline (Repsol-YPF) was as follows: aromatics, 69.8 wt.%; alkenes, 13.7 wt.%; dialkenes, 9.3 wt.%; cycloalkanes, 7.1 wt.%; isoalkanes, 5.0 wt.% and alkanes, 4.4 wt.%. The total sulfur content was 66 ppm and the density at 15 °C was 0.83 kg/L.

3. Results and discussion

3.1. Catalyst properties

Metallic properties (Pt content expressed as weight percentage on a water-free basis, dispersion and metal-particle diameter) and textural properties of the calcined catalysts are summarized in Table 1. Among the bifunctional catalysts, only Pt/Z19 shows platinum content close to its nominal value (0.5 wt.%). Pt/Z15 catalyst displays the highest metal dispersion and the highest metal exposure, as deduced from CO chemisorption results shown in Table 1. On the contrary, Pt/Z95 catalyst displays the lowest metal dispersion. The $Pt/\gamma\text{-}Al_2O_3$ catalyst, which was used for preparing the hybrid Pt/H15 catalyst, displays a relatively high dispersion, leading to Pt nanoparticles.

As seen in Table 1, the trend observed for the average pore diameter is: z15 ≫ Pt/Z15 > Pt/Z19 > Pt/Z95 which is opposite to that observed for the values of BET surface area of the catalysts. The acidic function z15 shows the lowest average pore diameter because the presence of binder and α-alumina contributes to enhancing macroporosity. It is noteworthy that an increase in the N_2 volume adsorbed at $P/P^0 = 0.2$ is observed simultaneously to an increase in the Si/Al ratio of the catalysts. Moreover, an increase in the average pore diameter is also observed (d_p, Table 1)

In this study, acid site strength and concentration in the catalysts were determined by a calorimetric study (TG-DSC) of NH_3 adsorption and desorption. NH_3 (cross-sectional area 0.14 nm^2) can diffuse through the pores of the HZSM-5 support (0.24 nm^2) and reach virtually all the acid sites. The classification of the acid sites has been carried out on the basis of an arbitrary range: weak (150–280 °C), medium (280–420 °C), and strong (420–550 °C).

Table 1
Platinum loading, metal dispersion and textural properties of the bifunctional catalysts and monofunctional z15 catalyst (used for hybrid Pt/H15).

Catalyst	Pt/Z15	Pt/Z19	Pt/Z95	z15	$Pt/\gamma\text{-}Al_2O_3$
Pt content (wt.%)[a]	0.38	0.52	0.33	–	0.51
Dispersion (%)[b]	23	19	14	–	85
d_p^M (nm)[b]	4.89	5.81	7.91	–	1.34
S_{BET} ($m^2\ g_{cat}^{-1}$)[c]	311	337	445	220	118
d_p (nm)[c]	3.1	2.9	2.5	8.6	9.1
$V_{P/P^0=0.2}$ (cm^3_{STP}/g_{cat})[c]	89	98	128	62	33
V_{pore} (cm^3_{STP}/g_{cat})[c]	0.24	0.24	0.28	0.40	0.26
$V_{\mu pore}$ (cm^3_{STP}/g_{cat})[c]	0.11	0.11	0.10	0.04	–

[a] Platinum loading as determined by ICP-AES of oxide precursors.
[b] Metal dispersion and Pt particle sizes (d_p^M) as determined by CO chemisorption of reduced catalysts.
[c] BET specific surface area (S_{BET}); average pore diameter (d_p); volume of N_2 adsorbed in total pores (V_{pore}), micropores ($V_{\mu pore}$) and at $P/P^0 = 0.2$, as measured by N_2 adsorption–desorption isotherms at −196 °C.

Table 2
Acidic properties of the reduced bifunctional catalysts and of the acidic function (z15) used for the hybrid catalyst.

Catalyst	Pt/Z15	Pt/Z19	Pt/Z95	z15
B:L[a]	3.02	3.64	0.92	2.62
Acidity ($\mu mol_{NH_3}/g_{cat}$)[b]	641	585	66	175
Weak ($\mu mol_{NH_3}/g_{cat}$)[b]	221 (52%)	97 (26%)	16 (25%)	83 (47%)
Medium ($\mu mol_{NH_3}/g_{cat}$)[b]	165 (39%)	186 (50%)	44 (67%)	84 (48%)
Strong ($\mu mol_{NH_3}/g_{cat}$)[b]	40 (9%)	89 (24%)	6 (9%)	8 (5%)

Percentage of the corresponding acid sites is given in parenthesis.
[a] Brønsted-to-Lewis acid site ratio, as determined by FTIR spectra of adsorbed pyridine at 150 °C.
[b] Total acidity and concentrations of the weak, medium and strong acid sites were determined by TG-DSC of adsorbed NH_3.

Table 2 compiles amount of weak, medium and strong acid sites obtained by such classification. As seen in this table, Pt/Z15 catalyst shows the largest amount of weak acid sites amongst the catalysts studied.

Considering the total amount of acid sites (Table 2, expressed as μmol of adsorbed NH_3 per gram of catalyst), the observed trend is: Pt/Z15 > Pt/Z19 ≫ z15 > Pt/Z95. However, we must consider that z15 catalyst contains 25 wt.% of pure zeolite HZSM-5. If we compare the values of acidity according to the amount of pure zeolite; z15 shows a value of ca. 700 $\mu mol_{NH_3}/g_{zeolite}$. In terms of acidity distribution (weak, medium or strong, Table 2) both catalysts Pt/Z15 and z15 display comparable contributions of each type of acidity.

Fig. 1 shows the acid strength distributions of the catalysts, as measured by calorimetric adsorption of NH_3. The comparison of the acid distribution of the acidic function (z15) with that of Pt/Z15 catalyst indicates that the addition of bentonite and α-alumina to the pure HZSM-5 does not change significantly the acid distribution. On the other hand, the adsorption profiles of Pt/Z15, Pt/Z19 and z15 catalysts show analogous acidic strengths of ca. 0.15 J/μmol_{NH_3}.

As the DSC-NH_3 technique did not allow for discriminating between Brønsted and Lewis acidities, FTIR spectra of adsorbed pyridine were recorded in order to obtain information on the relative proportion of the two types of acidic sites. Table 2 compiles the Brønsted-to-Lewis (B:L) acidity ratio, calculated using the areas under the bands at 1450 and 1550 cm^{-1}, associated with Lewis-type and protonated Brønsted-type pyridinium ions, respectively. The B:L acidity ratio follows the trend: Pt/Z19 > Pt/Z15 > z15 > Pt/Z95. The larger B:L acidity ratio of Pt/Z19 catalyst as compared to Pt/Z15 might indicate that some protons of the latter catalyst were not detectable. Indeed, the TG-DSC data recompiled in Table 2 clearly indicate that Pt/Z19 catalyst shows higher proportion of medium and strong acid sites compared to Pt/Z15 sample, which are normally associated with Brønsted acid sites.

3.2. Acidity-mechanism correlation

Fig. 2 displays the pyrolysis gasoline conversion at different H_2 pressures (ranging from 20 to 49 bar) as a function of the total acidity of the catalyst (measured by TG-DSC of adsorbed NH_3, Table 2). As seen in this figure, the conversion of pyrolysis gasoline depends linearly on the total amount of acid sites. The most active catalyst is the hybrid one since Pt/H15 displays the highest acidity per gram of zeolite (Table 2). Additionally, the result in Fig. 2 indicates that the increase in hydrogen pressure has a favourable effect on pyrolysis gasoline conversion, as observed before for the individual steps in the ring-opening of toluene and methylcyclohexane [15–17].

The increase in the activity of hydrocracking catalysts when support acidity is increased has been observed for catalysts with different metallic and acid functions and feeds of different composition [18–21].

It is noteworthy that total Pt dispersion (Table 1) increases in the same order as acidity (Table 2), however we did not find a linear correlation of the former with the pyrolysis gasoline conversion, in agreement with previous results [16]. This results leads to conclude that the larger Pt dispersion increases the metal surface available for aromatic hydrogenation, but as long as this reaction is considerably faster than cracking under these conditions, activity is mainly controlled by the acid properties of the catalyst.

Fig. 3 shows the influence of the catalyst and temperature on the Cracking Mechanism Ratio (CMR) defined as the yield proportion of isobutene over the products of monomolecular cracking (methane and ethane) [4,22]: $(Y_{C1} + Y_{C2})/Y_{iC4}$. As seen,

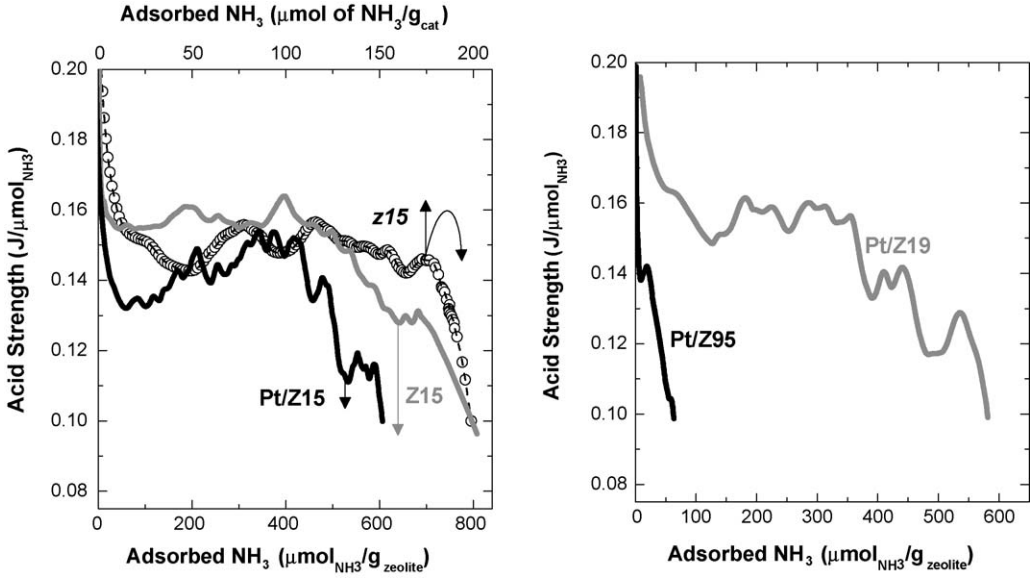

Fig. 1. Acid strength distribution of the bifunctional catalysts (reduced), acidic function z15 and pure support (Z15), as determined by TG-DSC monitoring of NH_3 adsorption at 150 °C.

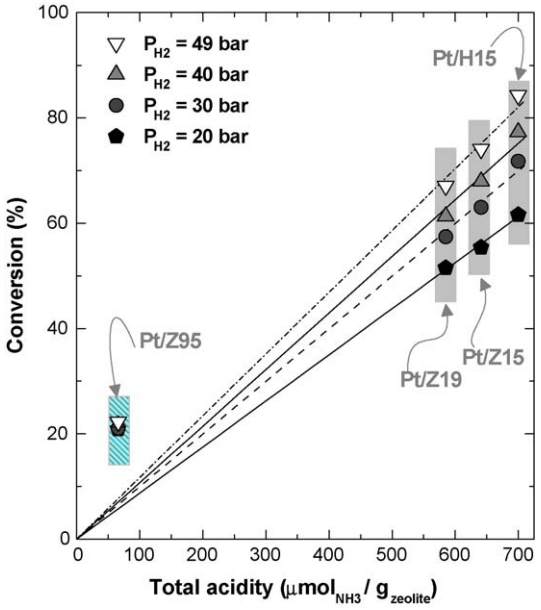

Fig. 2. Influence of catalyst acidity and H_2 pressure on pyrolysis gasoline conversion over bifunctional and hybrid catalysts. Reaction conditions: P_{H_2} = 49 bar, T = 350 °C and WHSV = 4 h^{-1}.

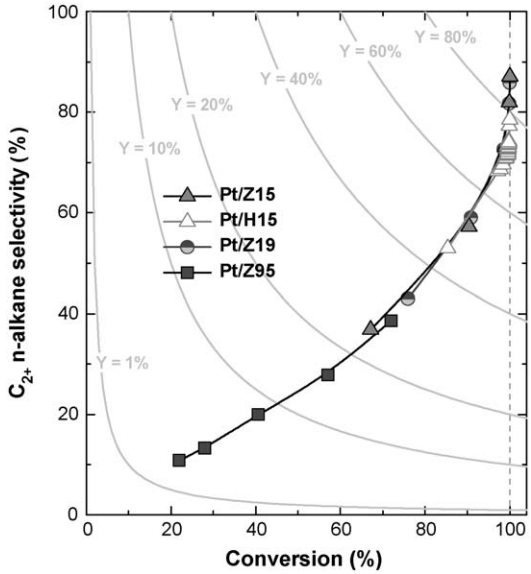

Fig. 4. Evolution of selectivity to C_{2+} *n*-alkanes with pyrolysis gasoline conversion (P_{total} = 50 bar, WHSV = 4 h^{-1}).

CMR increases linearly with temperature for all catalysts. This result is applicable in all cases excluding the data concerning Pt/Z95 catalyst at 350 °C, which are the conditions used for Fig. 2. Consequently, the deviation from linearity (in both Figs. 2 and 3) of Pt/Z95 catalyst at 350 °C is attributed to a change in the controlling mechanism; towards hydrogenolysis. Nevertheless, at temperatures higher than 400 °C all catalysts show that cracking is the controlling mechanism (Fig. 3). The higher impact of hydrogenolysis reactions on Pt/Z95 cannot be ascribed to Pt exposure since this catalyst exhibits the lowest values (Table 1). This effect is caused by a depletion of the reactions taking place on the support, due to the lower values in the number of acid sites (Table 2) and acid strength (Fig. 3).

Fig. 4 shows the influence of conversion extent on the selectivity to C_{2+} *n*-alkanes which can shade light on a change in the mechanisms responsible for C_{2+} *n*-alkanes formation. All the catalyst follow the same trend regardless the metal–support interaction and acidity, which is evidence that there is no significant change in the controlling mechanism. This result is due to the fact that the main reaction occurring on Pt/Z95 catalyst at low temperatures (350 °C) is endocyclic cracking, whereas the exocyclic cracking (responsible for C_{2+} *n*-alkanes formation) prevails on catalysts with higher acidity and/or at higher temperatures).

The results in Fig. 4 show that, for a family of catalysts prepared with the same acid function (same shape selectivity), product distribution changes with reaction extent (quantified by pyrolysis gasoline conversion), but the properties of the acid support, such as the Brønsted/Lewis ratio and the acid strength distribution, do not have a significant effect. This result confirms that obtained in the hydrocracking of toluene [7].

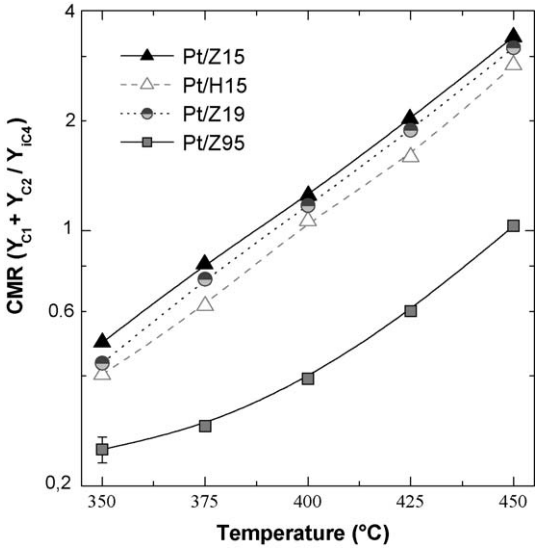

Fig. 3. Cracking Mechanism Ratio (CMR) as a function of temperature for the catalysts used. P_{H_2} = 49 bar, WHSV = 4 h^{-1}.

3.3. Effect of metal–support interaction on product selectivity

The joint effect of the metal–support interaction and catalyst acidity on methane and C_{2+} *n*-alkane yields are shown in Fig. 5a and b, respectively. As observed, the yields of methane and *n*-alkanes increase as hydrogen partial pressure is increased, which is a consequence of favouring protolytic cracking reactions. However, concerning the formation of C_{2+} *n*-alkanes (Fig. 5b), this increase in yield is less significant with the bifunctional catalysts of larger acidity (Pt/Z15). This is because the interaction between Pt and support is stronger on the support of largest amount of –OH groups. In such conditions, hydrogen "spill-over" is enhanced because the reactant molecules are strongly retained on the acid sites [23]. As a consequence, the kinetic performance of Pt/Z15 catalyst is less dependent on the hydrogen partial pressure than in case of Pt/Z19 and Pt/Z95 catalysts. Those results are consistent with the fact that, total acidity of the zeolite (Pt/Z15 > Pt/Z19) and not the concentration of Brønsted acid sites (Pt/Z19 > Pt/Z15), is the responsible for the hydrogenolytic cracking.

Pt/H15 catalyst has the largest acidity and the largest Pt exposure which make this catalyst the most active (Fig. 2). However, a higher proportion of alkanes–methane (Fig. 5) is

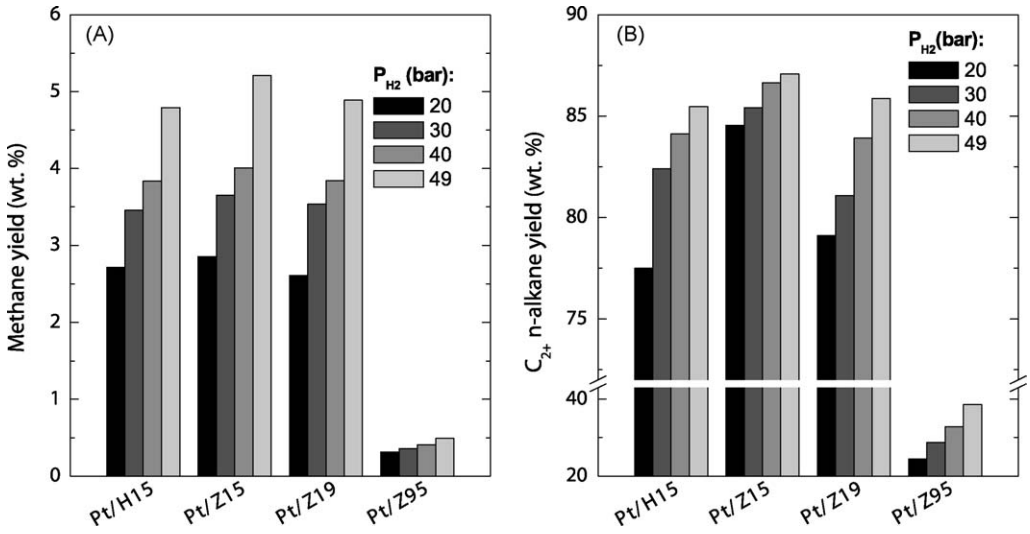

Fig. 5. Effect of the catalyst and P_{H_2} on the yields of methane (a) and C_{2+} *n*-alkane (b). T = 450 °C, WHSV = 4 h^{-1}.

obtained when a bifunctional catalyst (made with the same active species, Pt/Z15) is used; that is, a higher Pt–HZSM-5 interaction boosts the production of C_{2+} *n*-alkanes, minimizes the yield of methane, but reduces the requirements of hydrogen for a certain production of C_{2+} *n*-alkanes.

4. Conclusions

- The conversion of pyrolysis gasoline over Pt/HZSM-5 catalysts is linearly dependent on support acidity. At low acidity values the main mechanism for ring-opening is through hydrogenolysis and thus, the less acidic catalyst shows higher conversion than expected.
- The highest activity observed for Pt/H15 catalyst was explained by two factors: (i) the largest acidity linked with its lowest Si/Al ratio and (ii) the largest Pt dispersion, which increases the metal surface available for pyrolysis gasoline hydrogenation.
- Hybrid Pt/HZSM-5 catalyst, as compared to the bifunctional one, showed lower metal–support interaction but a higher catalytic activity. However, the bifunctional catalyst increases the ratio C_{2+} *n*-alkanes:methane but minimizes hydrogen requirements.
- Product distribution is a consequence of conversion level, but the properties of the acid function, such as the Brønsted/Lewis ratio and the acid strength distribution, do not have a significant effect.

Acknowledgements

The authors gratefully acknowledge the valuable comments and suggestions made by Jorge Vicente. This work has been carried out through the financial support of the Ministry of Education and Science of the Spanish Government (Project CTQ2006-03008) and of the University of the Basque Country and Basque Government (Department of Education, Universities and Research) (Project IT-220-07). P.C. wishes to thank the Basque Government (Department of Education, Universities and Research) for the Fellowship (BFI02.96).

References

[1] R.J. Beck, Oil Gas J. 18 (1999) 49.
[2] H. Du, C. Fairbridge, H. Yang, Z. Ring, Appl. Catal. A: Gen. 294 (2005) 1.
[3] C. Ringelhan, G. Burgfels, J.G. Neumayr, W. Seuffert, J. Klose, V. Kurth, Catal. Today 97 (2004) 277.
[4] J. Weitkamp, A. Raichle, Y. Traa, Appl. Catal. A: Gen. 222 (2001) 277.
[5] A. Raichle, Y. Traa, J. Weitkamp, Catal. Today 75 (2002) 133.
[6] Ullmann's Encyclopedia of Industrial Chemistry, 7th edition, John Wiley & Sons, Inc., New York, 2006.
[7] P. Castaño, B. Pawelec, A.T. Aguayo, A.G. Gayubo, J.M. Arandes, Ind. Eng. Chem. Res. 47 (2008) 665.
[8] P. Castaño, A. Gutiérrez, B. Pawelec, J.L.G. Fierro, A.T. Aguayo, J.M. Arandes, Appl. Catal. A: Gen. 333 (2007) 161.
[9] P. Castaño, B. Pawelec, J.L.G. Fierro, J.M. Arandes, J. Bilbao, Appl. Catal. A: Gen. 315 (2006) 101.
[10] M.A. den Hollander, M. Wissink, M. Makkee, J.A. Moulijn, Appl. Catal. A: Gen. 223 (2002) 85.
[11] C. Berger, A. Raichle, R.A. Rakoczy, Y. Traa, J. Weitkamp, Microp. Mesop. Mater. 59 (2003) 1.
[12] A. Raichle, Y. Traa, F. Fuder, M. Rupp, J. Weitkamp, Angew. Chem., Int. Ed. 40 (2001) 1243.
[13] A. Raichle, M. Ramin, D. Singer, M. Hunger, Y. Traa, J. Weitkamp, Catal. Commun. 2 (2001) 69.
[14] C.A. Emeis, J. Catal. 141 (1993) 347.
[15] P. Castaño, J.M. Arandes, B. Pawelec, M. Azar, J. Bilbao, Ind. Eng. Chem. Res. 47 (2008) 1043.
[16] P. Castaño, J.M. Arandes, B. Pawelec, J.L.G. Fierro, A. Gutierrez, J. Bilbao, Ind. Eng. Chem. Res. 46 (2007) 7417.
[17] P. Castaño, A.G. Gayubo, B. Pawelec, J.L.G. Fierro, J.M. Arandes, Chem. Eng. J. 140 (2008) 287.
[18] A.M. Alsobaai, R. Zakaria, B.H. Hameed, Fuel Proc. Technol. 88 (2007) 921.
[19] L. Ding, Y. Zheng, Z. Zhang, Z. Ring, J. Chen, Appl. Catal. A: Gen. 319 (2007) 25.
[20] S.K. Maity, G.A. Flores, J. Ancheyta, M.S. Rana, Catal. Today 130 (2008) 374.
[21] K.M. Cho, S. Park, J.G. Seo, M.H. Youn, S.H. Baeck, K.W. Jun, J.S. Cung, I.K. Song, Appl. Catal. B: Environ. 83 (2008) 195.
[22] A.F.H. Wielers, M. Vaarkamp, M.F.M. Post, J. Catal. 127 (1991) 51.
[23] D. Eliche-Quesada, M.I. Macías-Ortiz, J. Jiménez-Jiménez, E. Rodríguez-Castellón, A. Jiménez-López, J. Mol. Catal. A: Chem. 255 (2006) 41.